Supplemental data

Cdk4 deficiency augments *Myc*-driven lymphomagenesis via a Foxo1-Rag1/Rag2 pathway that provokes genomic instability

Yuanzhi Lu[1,5], Yongsheng Wu[1,5], Xiaoling Feng[1,5], Rulong Shen[1], Jing H. Wang[2], Mohammad Fallahi[3], Weimin Li[3], Chunying Yang[3], William Hankey[1], Ming O. Li[4], John L. Cleveland[3] and Xianghong Zou[1,6]

[1]Department of Pathology, Arthur G. James Comprehensive Cancer Center, The Ohio State University, Columbus, Ohio, USA
[2]Department of Genetics, Harvard Medical School, Boston, Massachusetts, USA
[3]Department of Cancer Biology, The Scripps Research Institute, Jupiter, Florida, USA
[4]Memorial Sloan-Kettering Cancer Center, 1275 York Avenue New York, New York, USA.

[5]These authors contributed equally to this work

[6]Correspondence to Xianghong Zou, 140 Hamilton Hall, 1645 Neil Avenue, Columbus, OH 43210. Phone: 614-688-8424; Fax: 614-292-7072; E-mail: zou.32@osu.edu

Supplementary information includes:

Supplemental Figures S1-S13 and Supplemental Figure Legends

Supplemental Tables S1-S5

Supplemental Methods

Supplemental References

Supplemental Figures with Legends

Supplemental Figure S1

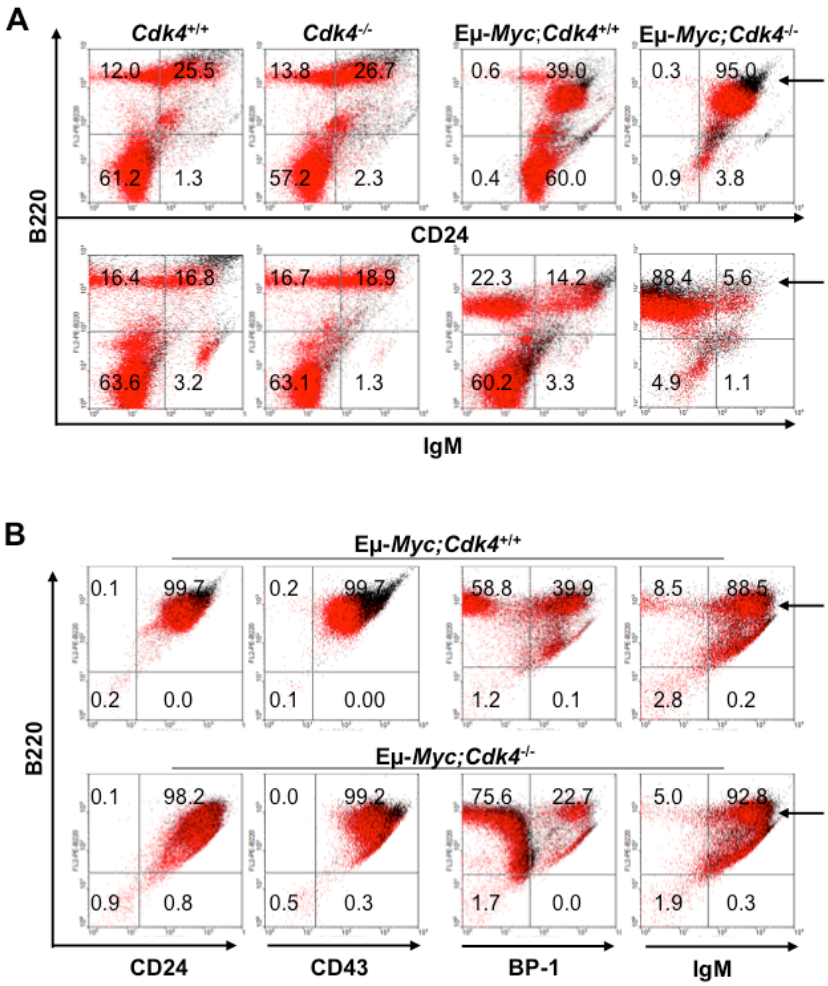

Supplemental Figure S1. Phenotype of lymphomas arising in Eμ-*Myc*;*Cdk4*$^{-/-}$ transgenics is comparable to those arising in Eμ-*Myc* transgenics. (**A**) Cells from the lymph nodes (LN) of the indicated mice (at 7 weeks of age) were stained with antibodies to B220, CD24, CD43, BP-1, or IgM and FACS analyses were performed. Percentages indicate cells in the gated live cell populations (data for CD43 and BP-1 are not shown). Using all markers, more than 90% of cells from the LN of Eμ-*Myc*;*Cdk4*$^{-/-}$ mice are B220+ (arrows), whereas LN of *Cdk4*$^{+/+}$, *Cdk4*$^{-/-}$, and Eμ-*Myc*;*Cdk4*$^{+/+}$ mice had only 34-40% total B220+ B cells. Results shown are representative of those obtained from 8 different mice in each cohort. Statistical analyses are provided in Figure 1C**.** (**B**) Cells were isolated from the enlarged LN of the indicated mice ≥ 12 weeks of age and were stained with antibodies to B-cell markers (B220, CD24, CD43, BP-1 and IgM) and analyzed by FACS. As in Eμ-*Myc*;*Cdk4*$^{+/+}$ mice, all cells from the lymphomas derived from Eμ-*Myc*;*Cdk4*$^{-/-}$ mice are B220+, confirming their B cell nature and were either immature or mature B cell lymphoma (see also Supplemental Table S2). Results shown are representative of those obtained from 8 different lymphomas for each cohort. n=8, mean±SD, p>0.5.

Supplemental Figure S2

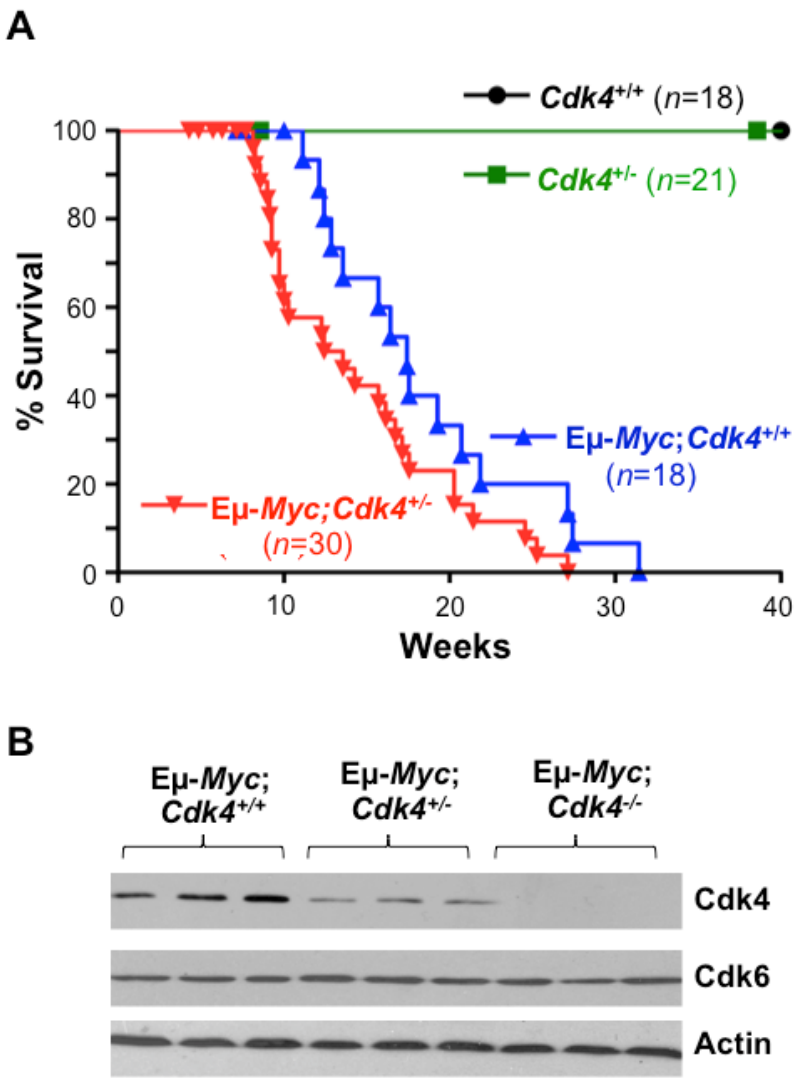

Supplemental Figure S2. (**A**) *Cdk4* heterozygosity accelerates Myc-induced lymphomagenesis. Kaplan-Meier survival curves of *Cdk4*$^{+/+}$, *Cdk4*$^{+/-}$, Eμ-*Myc*;*Cdk4*$^{+/+}$, and Eμ-*Myc*;*Cdk4*$^{+/-}$ littermates. *n* represents the numbers of mice in each group. Horizontal line indicates ages of surviving mice. $p<0.05$. The Eμ-*Myc*;*Cdk4*$^{+/-}$ cohort had a mean mortality of 13 weeks, whereas the Eμ-*Myc*;*Cdk4*$^{+/+}$ littermates display a typical survival curve, with a mean mortality of 18 weeks**.** (**B**) Cdk4 expression is significantly reduced in Eμ-*Myc*;*Cdk4*$^{+/-}$ lymphoma cells and Cdk6 expression is not altered by *Cdk4* deficiency of Eμ-*Myc* lymphomas. Lymphomas from Eμ-*Myc*;*Cdk4*$^{+/+}$, *Myc*;*Cdk4*$^{+/-}$ and Eμ-*Myc*;*Cdk4*$^{-/-}$ mice were assessed by immunoblotting with the indicated antibodies. The data shown are representative of three repeat analyses and similar findings were manifest in premalignant Eμ-*Myc*;*Cdk4*$^{+/+}$, Eμ-*Myc*;*Cdk4*$^{+/-}$ and Eμ-*Myc*;*Cdk4*$^{-/-}$ B cells.

Supplemental Figure S3

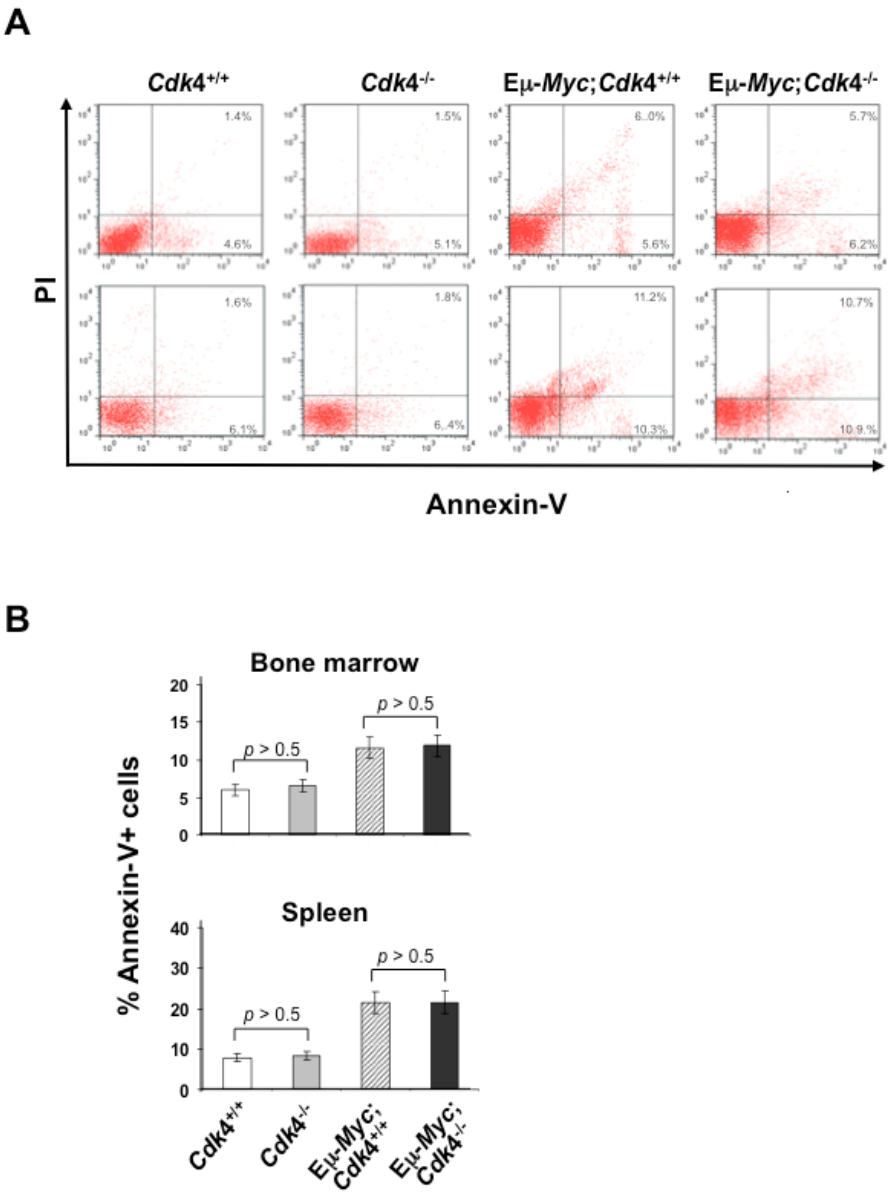

Supplemental Figure S3. Cdk4 deficiency does not affect the apoptotic index of premalignant Eμ-*Myc* B cells. (**A**) Premalignant B cells were isolated from bone marrow and spleens of 4-6 week-old *Cdk4*$^{+/+}$, *Cdk4*$^{-/-}$, Eμ-*Myc;Cdk4*$^{+/+}$ and Eμ-*Myc;Cdk4*$^{-/-}$ littermates and the apoptotic index was determined by FACS analyses of B220+ B cells by staining with anti-Annexin V-FITC and propidium iodide (PI). *Top*, representative FACS analyses for the indicated littermates are shown. (**B**) Quantification of the % Annexin-V+ B220+ B cells is shown for the indicated cohorts (*n=5; mean ±SD,* p*>0.5*).

Supplemental Figure S4

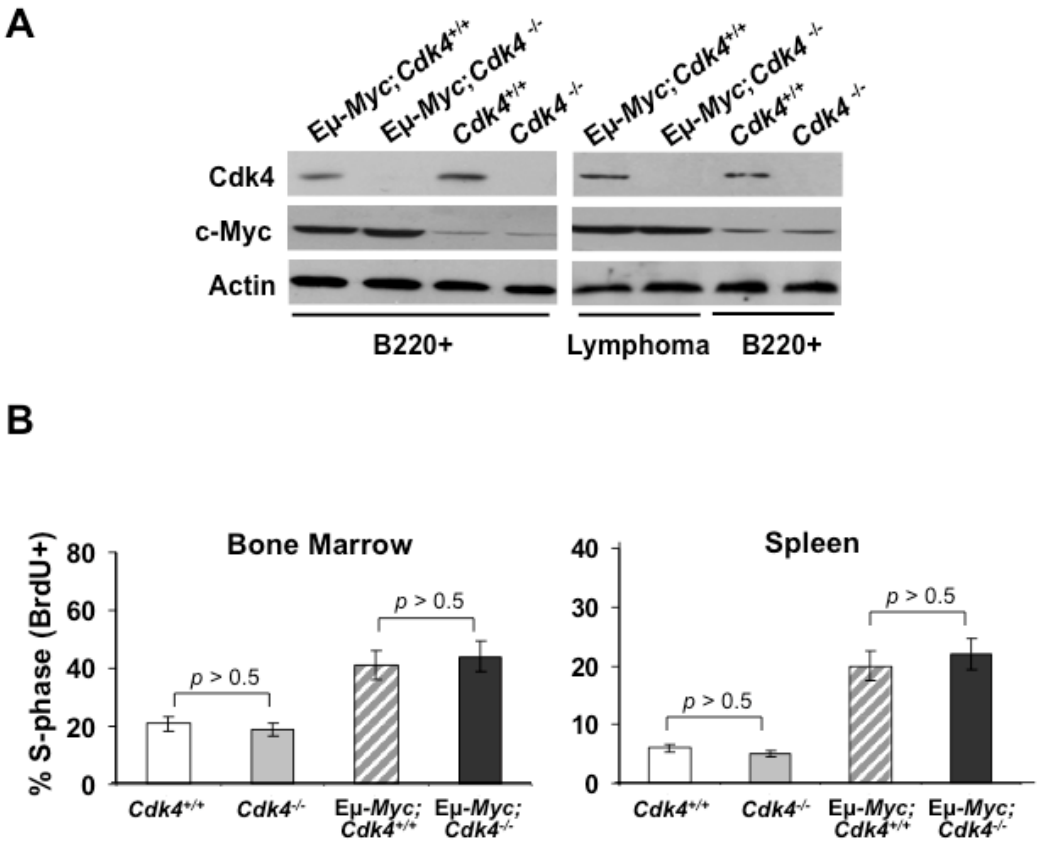

Supplemental Figure S4. (**A**) Levels of Cdk4 and c-Myc protein in precancerous bone marrow B220+ B-cells (*left panels*) or lymphomas (*right panels*) of Eμ-*Myc*;*Cdk4*$^{+/+}$ or Eμ-*Myc*;*Cdk4*$^{-/-}$ mice. Lysates from the LN of *Cdk4*$^{+/+}$ and *Cdk4*$^{-/-}$ littermates served as controls. Note that Cdk4 deficiency did not affect the elevated expression of the c-*Myc* transgene in Eμ-*Myc* B cells. Data shown is representative of three independent experiments and of six samples from each cohort. (**B**) The Cdk4 deficiency does not affect the proliferative status of premalignant Myc-expressing B cells. The indicated mice (4-6 week-old littermates) were injected with BrdU and after 12 hr bone marrow and spleen were harvested and the % BrdU+ B220+ B cells were determined by FACS. As expected Eμ-*Myc* B cells have marked increases in the numbers of B cells in cycle. However, this was not affected by *Cdk4* status.

Supplemental Figure S5

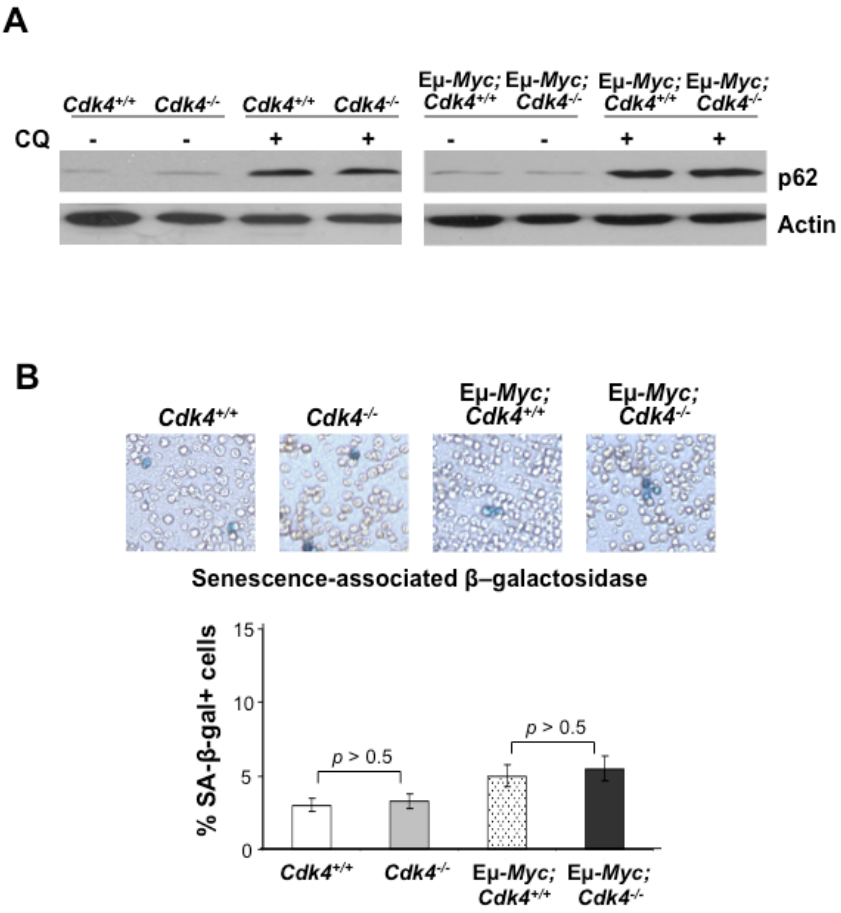

Supplemental Figure S5. (**A**) *Cdk4* status does not affect the expression of the autophagy substrate p62/Sequestrin. MACS-purified B220+ B cells of 4-6 week old wild type, *Cdk4*$^{-/-}$, Eμ-*Myc*;*Cdk4*$^{+/+}$ and Eμ-*Myc*;*Cdk4*$^{-/-}$ mice were cultured with or without chloroquine (CQ, 50 μM, Sigma) for 24 hr, and lysates then assessed by immunoblotting with anti-p62 antibody (MBL). Levels of p62/Sequestrin, a *bona fide* cargo of autophagosomes, were very low in B cells from all cohorts, and p62 levels were not affected by *Cdk4* status. However p62 levels were greatly induced, as expected, by chloroquine, which disrupts degradation of autophagosomal cargo by the lysosome. Data shown are representative of three independent analyses**.** (**B**) Cdk4 status does not affect senescence in Myc-expressing B cells. MACS-purified B220+ B cells of 4-6 week old wild type, *Cdk4*$^{-/-}$, Eμ-*Myc*;*Cdk4*$^{+/+}$ and Eμ-*Myc*;*Cdk4*$^{-/-}$ mice were stained with senescence-associated β-galactosidase (SA-β-gal) as described (1). Note that while there was a modest increase in the number of SA-β-gal-positive Eμ-*Myc* B cells there were no effects of Cdk4 deficiency. (*n*=5 random fields, 50-100 cells for each field, mean ±SD, *p*>0.5).

Supplemental Figure S6

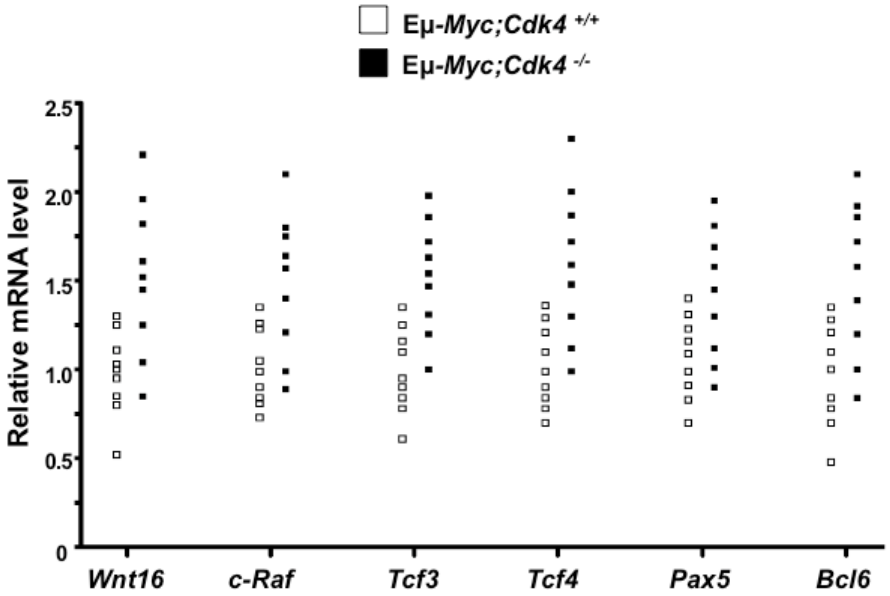

Supplemental Figure S6. Eμ-*Myc*;*Cdk4*$^{-/-}$ lymphomas express elevated levels of B cell malignancy-associated genes. Real-time qPCR analyses of the expression of the indicated genes from lymphomas arising in individual Eμ-*Myc*;*Cdk4*$^{+/+}$ (white rectangles) versus Eμ-*Myc*;*Cdk4*$^{-/-}$ (black rectangles) transgenics (*n*=9 for each cohort) is shown. As is evident, most Eμ-*Myc*;*Cdk4*$^{-/-}$ lymphomas expressed increased levels of *Wnt16*, *c-Raf* and *Tcf3*, *Tcf4*, *Pax5*, and/or *Bcl6* transcripts.

Supplemental Figure S7

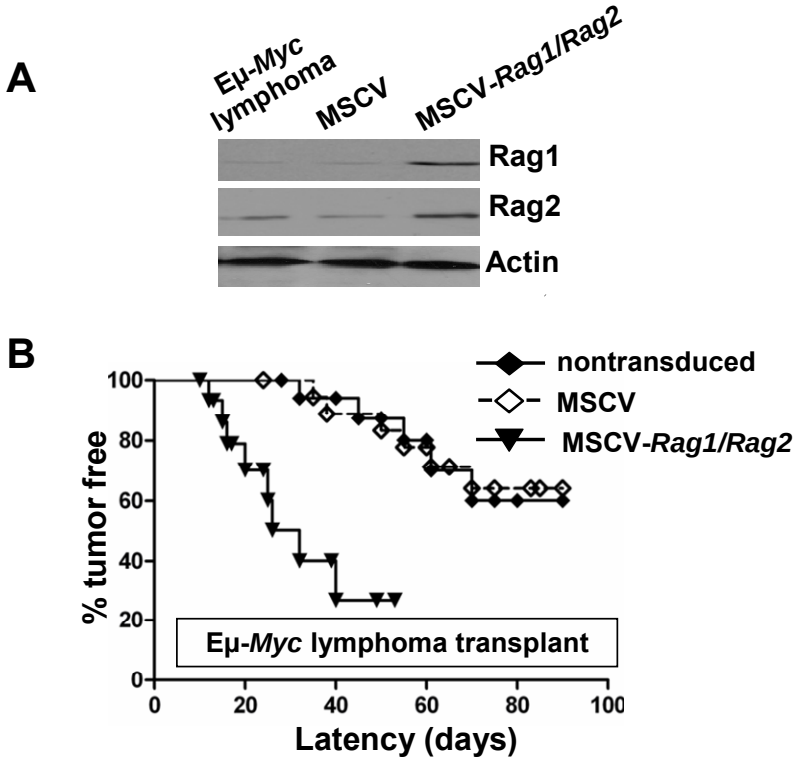

Supplemental Figure S7. Enforced co-expression of Rag1 and Rag2 expression augments tumorigenic potential of Eμ-*Myc* lymphoma. (**A**) Overexpression of Rag1 and Rag2 in Eμ-*Myc* lymphoma cells. Eμ-*Myc*;*Cdk4*$^{+/+}$ lymphoma cells (*n*=3 independent lymphomas) were transduced with MSCV-IRES-Puro control virus or were co-transduced with MSCV-Rag1-IRES-Puro (MSCV) and MSCV-Rag2-IRES-Hygro (MSCV-Rag1/Rag2) retroviruses. Lysates were then prepared from tranduced cells and assessed by immunoblotting with antibodies for Rag1, Rag2 and Actin. **(B)** Transduced Eμ-*Myc* lymphoma cells were transplanted into 6-8 week-old syngeneic C57Bl/6 recipients via tail vein injection and animals were observed daily for the development of lymphoma. Time to lymphoma onset is shown and is defined as the occurrence of palpable cervical or peripheral lymph nodes, at least 5 mm in one dimension. As is evident enforced co-expression of Rag1 and Rag2 augmented the tumorigenic potential of Eμ-*Myc* lymphoma (*n*=15, $p < 0.01$).

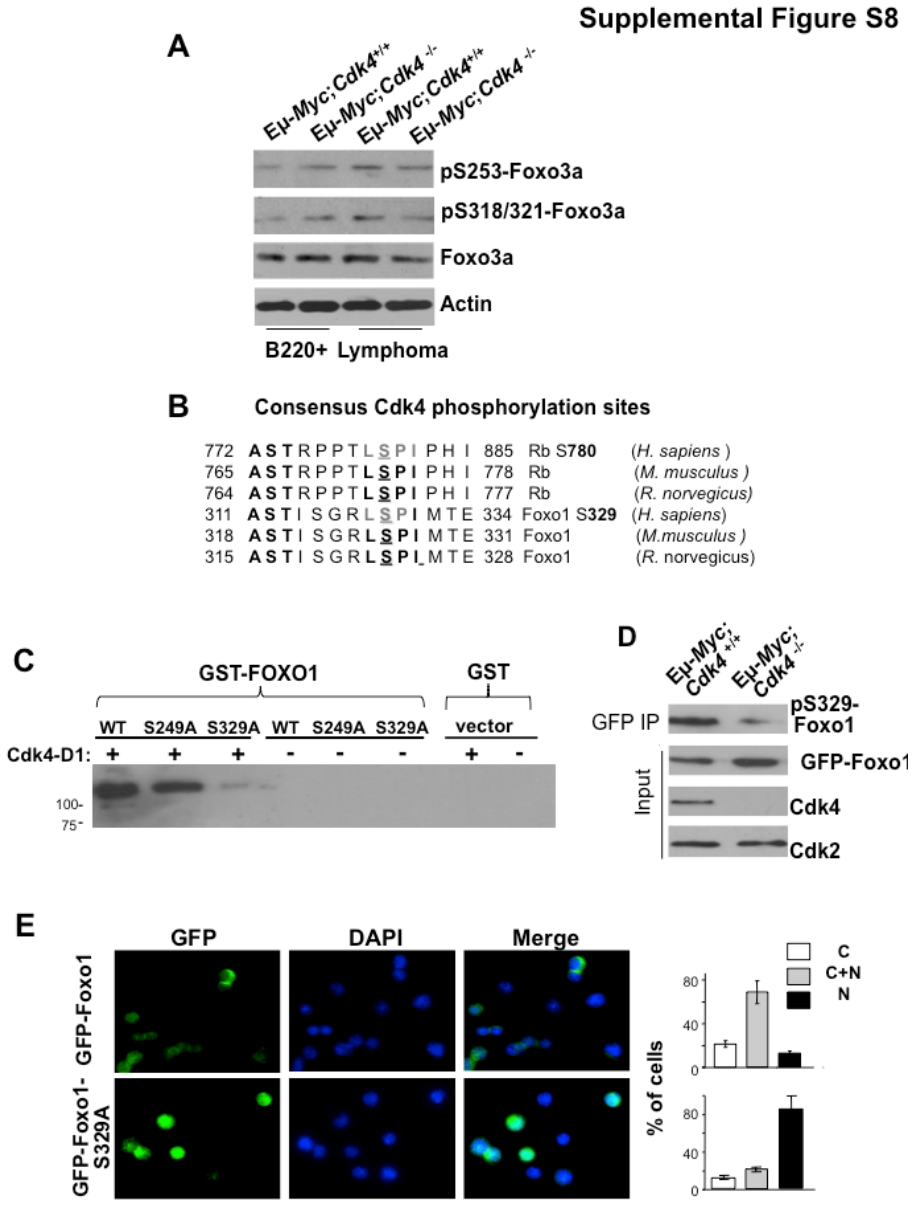

Supplemental Figure S8. (**A**) Cdk4 deficiency does not affect the steady state levels of Foxo3 or of pS253-Foxo3a or pS318/321-Foxo3a. Premalignant and neoplastic Eμ-*Myc*;*Cdk4*$^{+/+}$ and Eμ-*Myc*;*Cdk4*$^{-/-}$ B220+ B cells were assessed by immunoblotting with the indicated antibodies. Results shown are representative of three independent experiments. (**B**) Foxo1 harbors a putative Cdk4 phosphorylation site. A conserved putative Cdk4 motif is present in the forkhead domain of human, mouse and rat Foxo1, similar to the motif found in retinoblastoma protein (Rb), a Cdk4 substrate. Ser329 in man is Ser326 in mouse. (**C**) *In vitro* kinase assays using recombinant CyclinD/Cdk4 complexes and wild type (WT) Foxo1 or a Foxo1-S329A mutant fused to GST (GST-Foxo1). Note that wild type Foxo1 and Foxo1-S249A (a mutant that cannot be phosphorylated by Cdk2, ref. (2)) are phosphorylated by Cdk4, whereas Foxo1-S329A is weakly phosphorylated by Cdk4. (**D**) Lysates from Eμ-*Myc*;*Cdk4*$^{+/+}$ and Eμ-*Myc*;*Cdk4*$^{-/-}$ lymphoma expressing human GFP-Foxo1 fusion proteins were immunoprecipitated with GFP antibody and levels of GFP-pS329-Foxo1 levels were determined. Levels of total GFP-Foxo1, Cdk4 and Cdk2 were also determined. (**E**) Eμ-*Myc;Cdk4*$^{+/+}$ lymphoma expressing GFP-Foxo1 or GFP-Foxo1-S329A were assessed for localization of GFP-Foxo1 proteins. *Left panels*, GFP fluorescence; *Middle panels*, DAPI, *Right panels*, merge. Quantification of GFP-Foxo1 (*top graph*) or GFP-Foxo1-S329A (*bottom graph*) is shown at right (bar graphs). C, Cytoplasm; N, nucleus; C+N: C+N, cyt and nuc. Average of triplicate experiments is shown (*n*=100 for each cell type).

Supplemental Figure S9

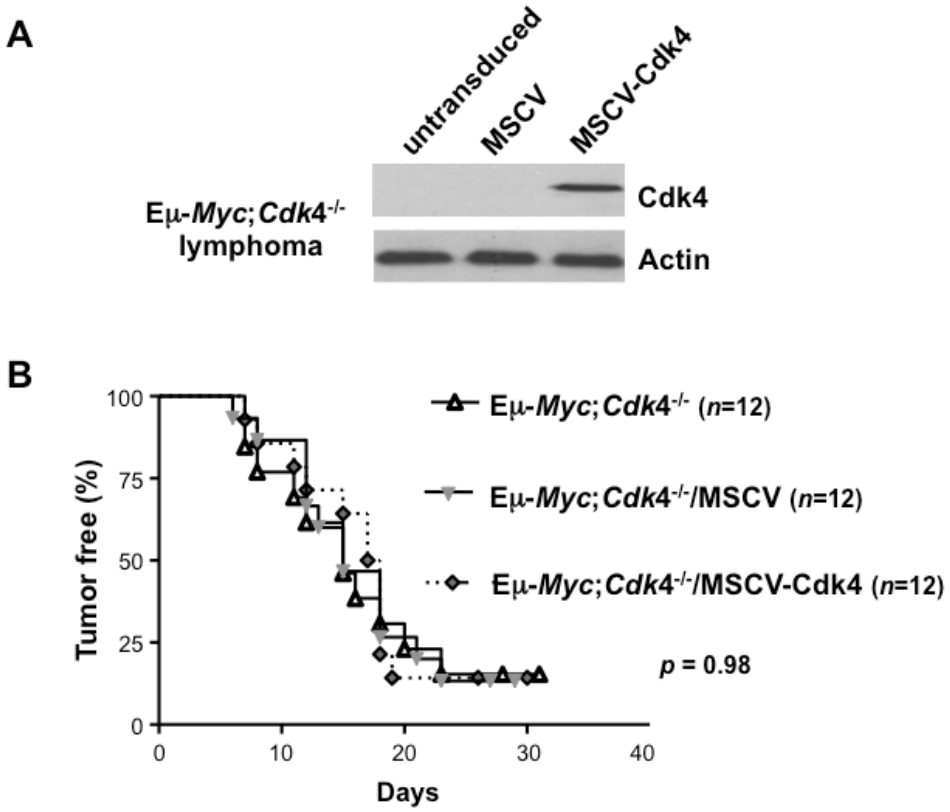

Supplemental Figure S9. Restoring Cdk4 expression does not affect the tumorigenic potential of Eμ-*Myc*;*Cdk4*$^{-/-}$ lymphoma. (**A**) Eμ-*Myc*;*Cdk4*$^{-/-}$ lymphoma cells were transduced with MSCV-IRES-Puro (MSCV) or MSCV-Cdk4-IRES-Puro (MSCV-Cdk4) retroviruses and transduced (Puro resistant) tumor cells were assessed by immunoblotting with antibodies that detect Cdk4 and Actin. (**B**) Lymphoma onset in recipients transplanted with Eμ-*Myc*;*Cdk4*$^{-/-}$ lymphoma transduced with MSCV *vs.* MSCV-Cdk4 retroviruses. Lymphoma onset is defined as the occurrence of palpable cervical or peripheral lymph nodes, at least 5 mm in one dimension. Statistical evaluation of tumor onset data is based on the log-rank (Mantel-Cox) test for comparison of the Kaplan-Meier event-time format, and on the unpaired *t* test for comparison of means and SD. $n = 12$; $p > 0.5$.

Supplemental Figure S10

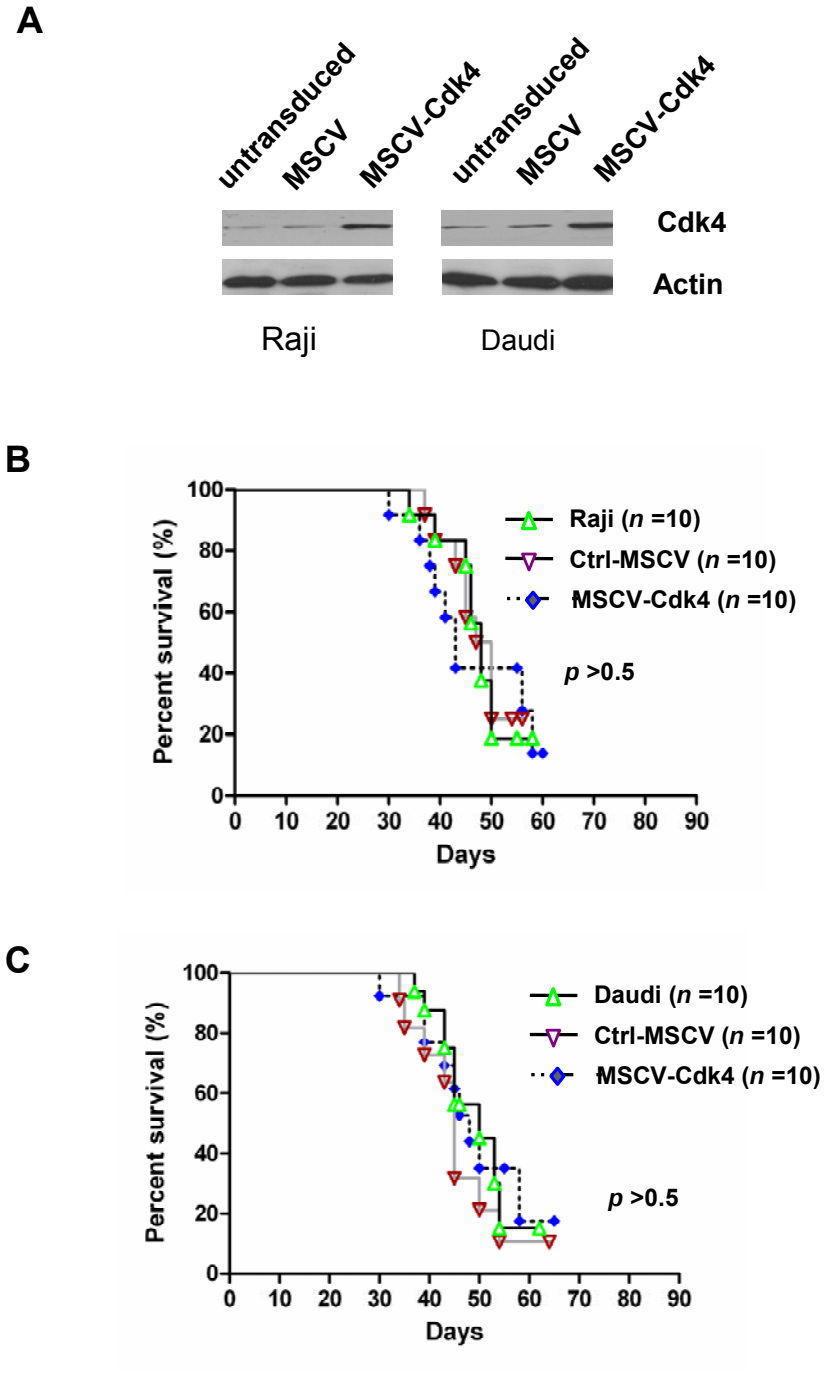

Supplemental Figure S10. Increased Cdk4 expression does not affect the tumorigenic potential of human B lymphoma cells (**A**) Raji or Daudi Burkitt lymphoma cells were transduced with MSCV-IRES-Puro (MSCV) or MSCV-CDK4-IRES-Puro (MSCV-CDK4) retroviruses and transduced tumor cells were assessed by immunoblotting with antibodies that detect CDK4 and Actin. (**B, C**) Lymphoma onset in *Nude* recipient mice transplanted with Raji (B) or Daudi (C) lymphoma cells transduced with MSCV *vs.* MSCV-CDK4 retroviruses. Lymphoma onset is defined as the occurrence of palpable cervical or peripheral lymph nodes, at least 5 mm in one dimension. Statistical evaluation of tumor onset data is based on the log-rank (Mantel-Cox) test for comparison of the Kaplan-Meier event-time format, and on the unpaired *t* test for comparison of means and SD. n = 10; p>0.5.

Supplemental Figure S11

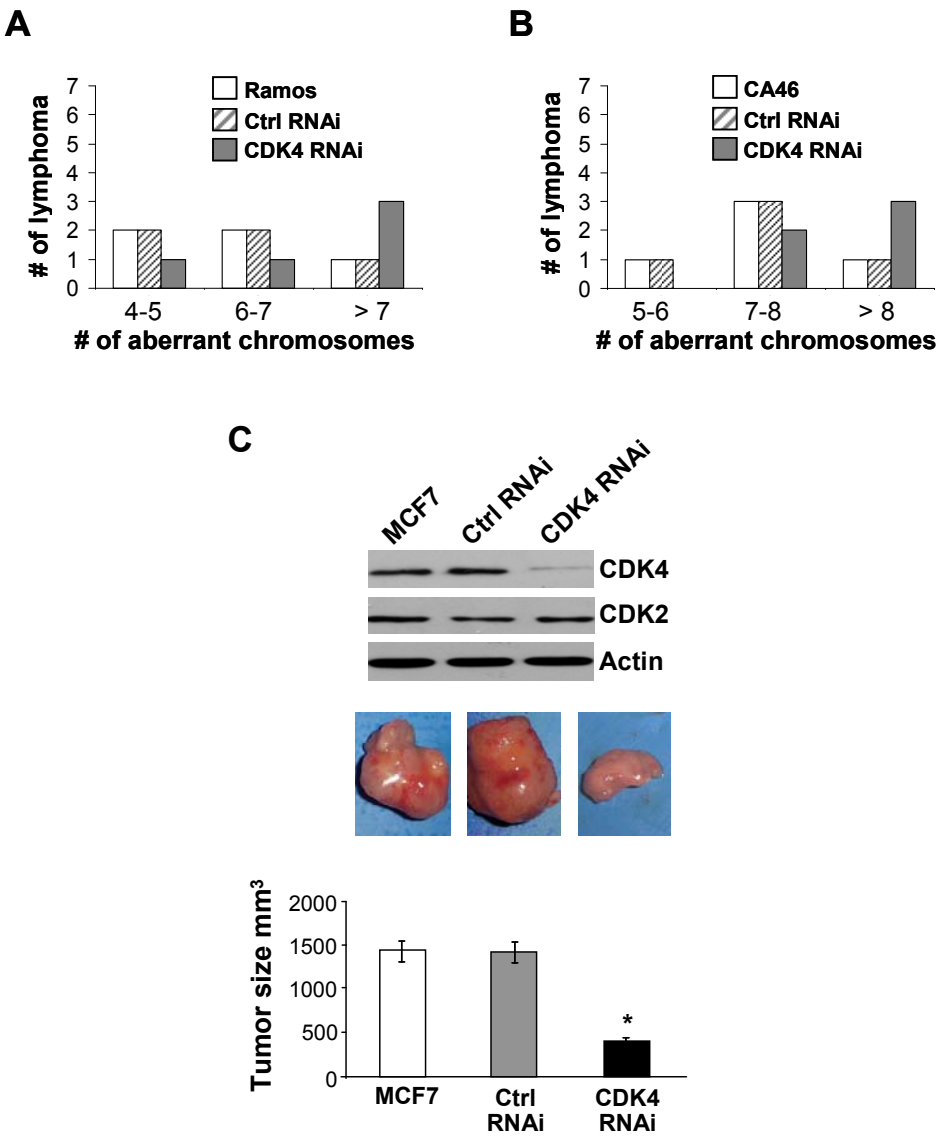

Supplemental Figure S11. (**A**, **B**) Knockdown of CDK4 augments genomic instability in human BL tumors. Lymphomas arising in *Nude* mice following transplant of control Ramos (**A**) and CA46 (**B**) BL cells or these BL cells stably expressing control RNAi or CDK4 RNAi were assessed from chromosomal alterations by karyotype analyses. Numbers of aberrant chromosomes are indicated. (**C**) Silencing CDK4 impairs the tumorigenic potential of MCF7 human ER+ breast cancer cells. *Top*, western blot of MCF7 cells with stable knockdown of CDK4. These MCF7 cells, those bearing control RNAi and untransfected parental MCF7 cells were transplanted (via subcutaneous injection) into 6-8 week-old *Nude* mice treated with β-estradiol slow-release pellets. 8 weeks after transplantation tumor sizes were determined (n=6 mice for each group; mean ± SD; *p<0.005). Representative images of tumors in the three cohorts are shown.

Supplemental Figure S12

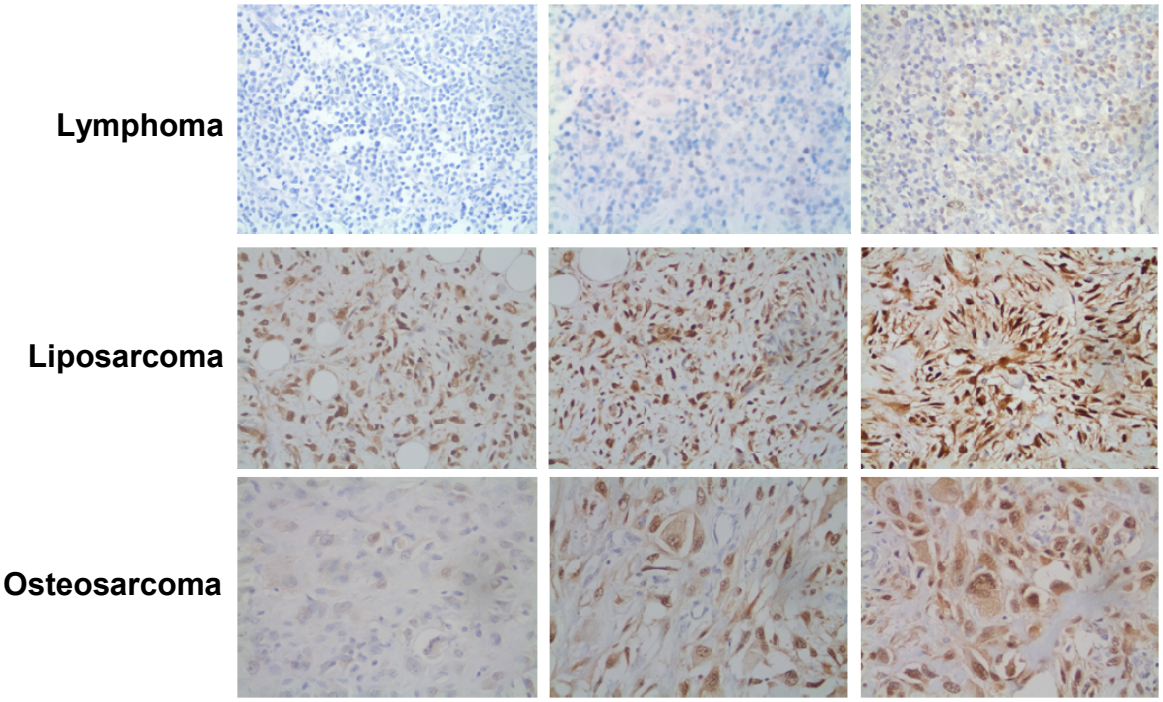

Supplemental Figure S12. Comparison of CDK4 expression in human B lymphoma versus other cancer types by immunohistochemistry analyses. Among all B cell lymphoma samples approximately 90% human B lymphoma samples have no or very low CDK4 expression (see Supplementary Table S5), whereas CDK4 levels were moderate-to-high in all liposarcomas or osteosarcomas analyzed. Magnification 400X.

Supplemental Figure S13

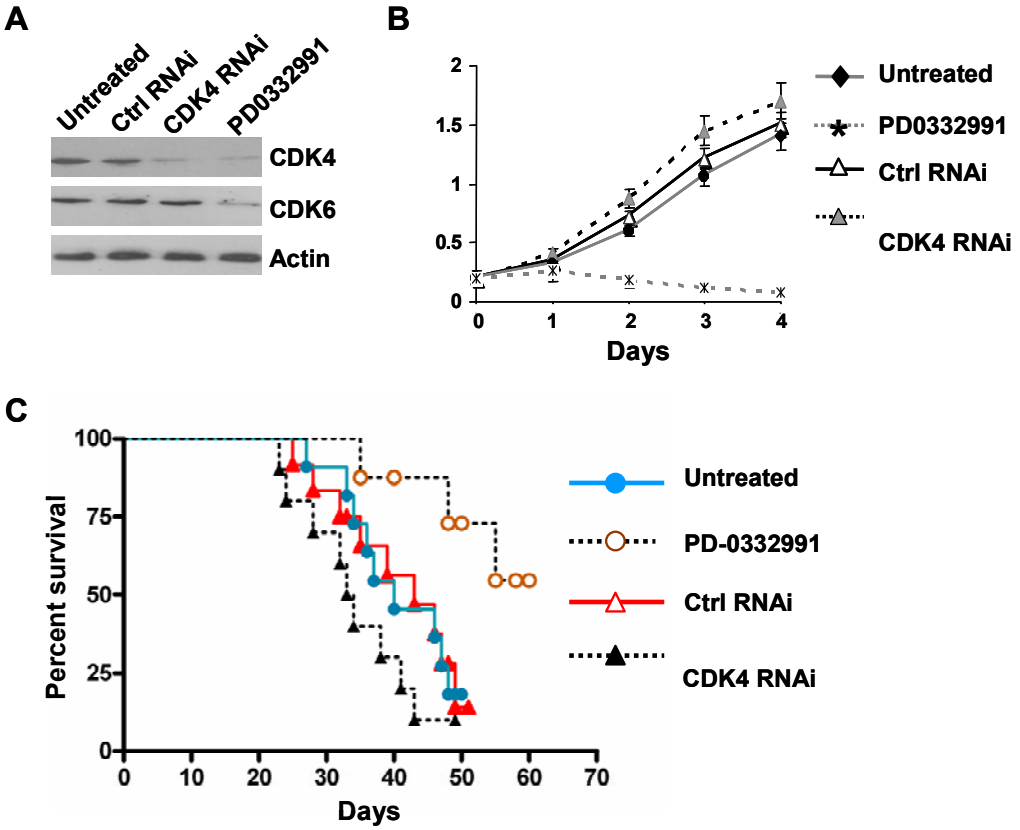

Supplemental Figure S13. Comparison of the effects of knockdown of CDK4 (by stable expression of RNAi) *vs.* treatment with the CDK4/CDK6 inhibitor PD0332991, on the tumorigenic potential of human Burkitt lymphoma (BL) cells. (**A**) Knockdown of CDK4 in the human Ramos BL cells. There were no changes in the levels of CDK6 following CDK4 knockdown by CDK4-RNAi. Surprisingly, treatment with PD0332991 inhibited the levels of both CDK4and CDK6. (**B**) Cell growth curve *ex vivo*. The cell lines (wild type Ramos BL cells, and these cells expressing stable CDK4-RNAi or harboring control-RNAi) were plated at a density of $2x10^5$ cells per well of a 96-well plate. PD0332991 (0.5-1 μM) or vehicle were added daily and cell number was determined at the indicated intervals (*n*=5 for each cohort). (**C**) $5x10^6$ Ramos BL cells (wild type, CDK4 knockdown or control RNAi) were transplanted into 6-8 week-old *Nude* mice. A cohort of recipient mice were treated with PD00332991 or vehicle when average tumor volume per experimental cohort reached 100 mm (refs. 3, 4, approximately 10 day following inoculation). Knockdown of CDK4 augmented the tumorigenic potential of lymphoma cells, while treatment with the PD0332991 inhibitor impaired tumorigenic potential (p=0.019). The contrasting effects of PD0332991 may reflect its dual activity versus CDK4 and CDK6, which appears to provoke unique vulnerabilities (refs. 4-7), or that it has targets in addition to CDK4 and CDK6, as limited kinase profiling (38 kinases) has been performed with this inhibitor (8). In accord with this notion, there were marked effects of PD0332991 on the steady state levels of both CDK4 and CDK6 in treated cells, suggesting a broader effect on signaling kinases. Similar findings were observed in studies with CA46 BL cells (not shown).

Supplemental Tables

Supplemental Table S1

Generation of Eμ-*Myc;Cdk4*$^{-/-}$ mice. To test the role of Cdk4 in Myc-driven lymphomagenesis, Eμ-*Myc*;*Cdk4*$^{-/-}$ mice were generated. Female Eμ-*Myc*;*Cdk4*$^{+/-}$ had reduced fecundity and died relatively early in life (though not as early as female Cdk4-deficient Eμ-*Myc* mice, not shown). Thus, female *Cdk4*$^{+/-}$ mice were crossed to male Eμ-*Myc*;*Cdk4*$^{+/-}$ transgenics to generate the desired cohorts: Eμ-*Myc*;*Cdk4*$^{+/+}$, Eμ-*Myc*;*Cdk4*$^{+/-}$, Eμ-*Myc*;*Cdk4*$^{-/-}$, *Cdk4*$^{+/+}$ and *Cdk4*$^{-/-}$ mice. Of 1896 mice produced by intercrossing, 118 Eμ-*Myc*;*Cdk4*$^{-/-}$ mice were born, which were used for the experiments presented herein.

Genotype	Number of mice	% of mice	
		Observed	Predicted
Cdk4$^{+/+}$	337	17.8	12.5
Cdk4$^{+/-}$	548	28.9	25
Cdk4$^{-/-}$	142	7.5	12.5
Eμ-*Myc*;*Cdk4*$^{+/+}$	271	14.3	12.5
Eμ-*Myc*;*Cdk4*$^{+/-}$	480	25.3	25
Eμ-*Myc*;*Cdk4*$^{-/-}$	118	6.2	12.5
Total	1896		

Supplemental Table S2

Phenotype of lymphomas arising in Eμ-*Myc*;*Cdk4*$^{+/+}$ *vs.* Eμ-*Myc*;*Cdk4*$^{-/-}$ mice.

Genotype	Number	Phenotype
Eμ-*Myc*;*Cdk4*$^{+/+}$	8	B220^{+} CD43^{+} BP-1^{-} (BP-1^{+}) CD24^{+} IgM^{+}
	4	B220^{+} CD43^{+} BP-1^{-} (BP-1^{+}) CD24^{+} IgM^{-}
	2	B220^{+} CD43^{+} BP-1^{-} CD24^{+} IgM^{+}
	2	B220^{+} CD43^{+} BP-1^{-} CD24^{+} IgM^{-}
Eμ-*Myc*;*Cdk4*$^{-/-}$	9	B220^{+} CD43^{+} BP-1^{-} (BP-1^{+})BCD24^{+} IgM^{+}
	3	B220^{+} CD43^{+} BP-1^{-} (BP-1^{+})CD24^{+} IgM^{-}
	1	B220^{+} CD43^{+} BP-1^{-} CD24^{+} IgM^{+}
	3	B220^{+} CD43^{+} BP-1^{-} CD24^{+} IgM^{-}

Lymphomas arising in 18 Eμ-*Myc*;*Cdk4*$^{+/+}$ and 16 Eμ-*Myc*;*Cdk4*$^{-/-}$ mice were immunophenotyped by flow cytometry using antibodies that detect B220, CD43, BP-1, CD24 and IgM.

Supplemental Table S3

Aberrant chromosome number and genomic instability in Eμ-*Myc*;*Cdk4*$^{-/-}$ *vs.* Eμ-*Myc*;*Cdk4*$^{+/+}$ lymphoma

Genotype	Sample list	Genomic gain	Genomic loss	Total aberrant Chr
Eμ-*Myc*;*Cdk4*$^{+/+}$	#1	Chr 5, 6		2
	#2	Chr 6		1
	#3	Chr 5	Chr 6	2
	#4	Chr 5, 6, 19		3
	#5	Chr 5, 6		2
	#6	Chr 5, 12, 19	Chr 6	4
Eμ-*Myc*;*Cdk4*$^{-/-}$	#7	Chr 6, 12	Chr12, 18	3
	#8	Chr 3, 19	Chr 3, 12, 16, X	5
	#9	Chr 6, 12, 18	Ch12, X	4
	#10	Chr 3, 6, 12, 18	Chr 3, 12, 19	5
	#11	Chr 6,12, 18, 19	Chr12	4
	#12	Chr 6, 12, 8, 19	Ch12, X	4

B220+ cells purified from lymphomas arising in Eμ-*Myc*;*Cdk4*$^{+/+}$ and Eμ-*Myc*;*Cdk4*$^{-/-}$ littermates (6 random pairs) were analyzed by karyotyping (see Figure 3A and 3B for typical metaphase spreads). Chromosome (Chr) regions that were prone to genomic instability (deletions, translocations, etc) and total number of aberrant chromosomes per lymphoma are also described in the legend to Figure 3.

Supplemental Table S4

Augmented activity of the Rag1/Rag2 complex in Eμ-*Myc*;*Cdk4*$^{-/-}$ lymphomas and in Rag1/Rag2-expressing Eμ-*Myc* lymphomas provokes cleavage and deletions at fortuitous RSSs within the *Bcl11b* gene.

	Junction	Intron 1	P and N nucleotides	Intron 3
WT		GACACACAGACACACAGA CACACACACACAC		CACTGTG TGAGATTAATTTCTTTCCT
(**A**) **Eμ-*Myc;Cdk4* $^{+/+}$ Lymphomas**				
WL1	-			
WL2	-			
WL3	+	GACACACAGACACACAGAC	GGGAAG	AATTTCTTTCCT
WL4	-			
WL5	-			
WL6	-			
(**B**) **Eμ-*Myc;Cdk4* $^{-/-}$ Lymphomas**				
KL1	+	GACACACACGACACACAGACAC	GG	GATTAATTTCTTTCCT
KL2	-			
KL3	+	GACACACAGACACACAGAC	GGA	TTAATTTCTTTCCT
KL4	-			
KL5	+	GACACACAGACACACAGAC	CC	AGATTAATTTCTTTCCT
KL6	+	GACACACAGACACACAGAC	CGAAG	TGAGATTAATTTCTTTCCT
(**C**) **Lymphomas arising in recipient mice engrafted with Eμ-*Myc* HSCs transduced with MSCV control virus**				
CH1	+	GACACACAGACACACAGACACAC	GGACG	TAATTTCTTTCCT
CH2	-			
CH3	-			
CH4	-			
CH5	-			
CH6	-			
(**D**) **Lymphomas arising in recipient mice engrafted with Eμ-*Myc* HSCs transduced with MSCV-*Rag1* and MSCV-*Rag2* virus**				
RH1	+	GACACACAGACACACAGACA	TGAGG	GATTAATTTCTTTCCT
RH2	-			
RH3	+	GACACACAGACACACAGACAC	CC	TGAGATTAATTTCTTTCCT
RH4	+	GACACACAGACACACAGAC	GGGA	GATTAATTTCTTTCCT
RH5	+	GACACACAGACACACAGACACAC	CC	AGATTAATTTCTTTCCT
RH6	+	GACACACAGACACACAGAC	CGAAG	TGAGATTAATTTCTTTCCT

Rag1/Rag2-mediated breakpoints in the *Bcl11b* loci are clustered in a region between *Bcl11b* intron 1 and intron 3 (9, 10). A nested PCR assay was performed to detect internal deletions in the *Bcl11b* major breakpoint region as described (9, 10), using the intron 1 F1 primer (5'-GGCTGAATTTACAGGATGAGG-3') and the R1 primer (5'-ACTGGAGTTTCCGATGGCC-3') of intron 3 (11, 12). **+** indicates breakpoint junction (positive PCR product). **-** indicates no breakpoint junction (no PCR product). As noted, 5 of the 6 lymphomas arising in recipient mice engrafted with Eμ-*Myc* HSCs engineered to co-express Rag1 and Rag2 yielded PCR products (**B**), while only one of the lymphomas arising in recipient mice engrafted with Eμ-*Myc* HSCs transduced with vector-only (control) had such a breakpoint (**A**). Notably, there are more internal deletions of *Bcl11b* manifest in Eμ-*Myc*;Cdk4$^{-/-}$ (**D**) versus Eμ-*Myc*;Cdk4$^{+/+}$ lymphomas (**C**). DNA sequences of the breakpoint junctions of *Bcl11b* deletions in these lymphomas are provided. Non-germline sequences are indicated in the center: N, non-templated; P, palindromic nucleotides. Underlined sequences indicate the conserved heptamer and a related cryptic motif, CA repeats. As expected, the sequencing of the PCR products revealed the presence of cryptic sequences recognizable by the Rag1/Rag2 recombinases near the breakpoints; *i.e.,* the heptamer sequence CACAGTG in intron 3 and a cryptic Rag1/Rag2 recognition sequence, CACA, in intron 1 (underlined) (12-14).

Supplemental Table S5

Immunohistochemical analyses of CDK4 expression of in human B cell lymphoma subtypes

Lymphoma type	±	+	++	+++	++++	Total cases
Non-Hodgkin lymphoma						
MALT-NHL	3	7	1	1	0	**12**
FL	12	11	1	1	0	**25**
DLBCL	33	30	3	1	1	**67**
BL	4	3	0	1	0	**8**
Hodgkin lymphoma						
cHL	0	2	0	2	1	**5**
LPHL	1	1	1	1	0	**4**
Other	1	3	0	0	0	**4**

Abbreviations: MALT-NHL, Malt-non-Hodgkin lymphoma (NHL); FL, Follicular Lymphoma; DLBCL, Diffuse large B-cell lymphoma; BL, Burkitt Lymphoma; cHL, Classical Hodgkin lymphoma; LPHL Lymphocyte-Predominant Hodgkin's Lymphoma.

CDK4 Staining: ±, no staining; +, weak staining; ++, moderate staining; +++, strong staining; and ++++, very strong staining.

Note: approximately 61% of the tested Non-Hodgkin lymphoma samples (68 of 112 NHL, including 42 DLBCL, 15 FL, 7 MALT-NHL, and 4 MALT-NHL) have high levels of c-Myc expression compared that B cells in control normal human LN.

Supplemental Methods

RNA preparation and real-time PCR. Total RNA was prepared from lymphoma cell lines and frozen tumors using TRIzol reagent (Invitrogen, Carlsbad, CA). First-strand cDNA was synthesized from total RNA with SuperScript (Invitrogen) according to the manufacturer's instructions. Real-time quantitative RT-PCR (qRT-PCR) analysis was performed on the ABI Prism 7000 sequence detection system (Applied Biosystems). The specific primers are as follows: *Rag1*, (CTGCAGACATTCTAGCACTC (5' primer) and AACTGAAGCTCAGGGTAGAC (3' primer); *Rag2*, CCTTCAGTGCCAAAATAAGA (5' primer) and TCATTAAGTGAGAAGCCTGGT (3' primer); *CD19***,** AATCCACGCATTCAAGTCCAG (5' primer) and GAGCCCTCCTCGCTGTCTG (3' primer); *p27*, CAGCTTGCCCGAGTTCTACT (5' primer) and GAGTTTGCCTGAGACC CAAT (3' primer); *Arf*, GCTCTGGCTTTCGTGAACATG (5' primer) and TCGAATCTGCACCGTAGTTGAG (3' primer)**,** *Wnt16***,** CTCGGATGATGTCCAGTACG (5' primer) and TCATGGCTAGCAGGACTCTG (3' primer); *c-Raf*, CATTGTTCAGCAGTTTGGCT (5' primer) and CATTGACCACAGTCCTTTGC (3' primer); *Tcf3*; CAGACACAGTCTCAGCAGCA (5' primer) and GGGCTATCACAAGGCTTCTC (3' primer); *Tcf4,* TTTGCCGTCTTCAGTCTACG (5' primer) and GCATGAAGAAGGAGCTAGGG (3' primer); *Pax5*, GATTCTTGGAGGTTCCCCAAC (5' primer) and GGGCTGCAGGGCTGTAATAG (3' primer)**;** *Bcl6*, GAGAAGCCATACCCCTGTGA (5' primer) and TGCACCTTGGTGTTTGTGAT (3' primer); *p53*, CGGGTGGAAGGAAATTTGTA (5' primer) and TGGATGGTGGTATACTCAGAGC (3' primer). The relative expression levels were calculated using the Comparative Cycle Threshold (CT) Method ($2^{-\Delta Ct}$) (Applied Biosystems).

The modified sequence of anti-Cdk4 siRNA was 5'AGCAACCACTGGAGGTGAAGT 3'. RNAi-resistant Foxo1-RE constructs, as well as Foxo1-siRNA were generated as described (2, 15).

Retrovirus and pLentvirus preparation. Retrovirus stocks were generated according to the manufacturer's protocol, and viral supernatants were collected 48 hr later and filtered before use as described previoulsy (1, 16). The pLentivirus preparation and infection in cells were performed following the protocol of the BLOCK-iT^{TM} Lentiviral RNAi (Invitrogen) with minor modifications. Briefly, after obtaining high titer stocks from 293T

packaging cells, lymphoma cells were transduced in 24-well plates by resuspending the cells ($5x10^4$ cells/ well) in 0. 5 ml of virus supernatants. The plate was then centrifuged at 4^oC at 1800 rpm for 45 min. 12 hr after infection the medium was changed to virus-free RPMI 1640 containing 10% FBS, and antibiotic selection (2-5 μg/ml blasticidin) was initiated following an additional 2-day recovery. After cell selection and expanding for one week, expression level of each target gene was analyzed by immunoblotting or qRT-PCR.

Chromatin immunoprecipitation. Thymocytes were fixed for 10 min at room temperature with 10% formaldehyde. After incubation, glycine was added to a final concentration of 0.125 M to “quench” the formaldehyde. Cells were pelleted, washed once with ice-cold PBS, and then lysed. The lysates were pelleted, resuspended and sonicated to reduce DNA length to between 500 and 1000 base pairs. Chromatin was precleared with protein A agarose beads for 1 hr and then incubated with 5 μg of Foxo1 antibody (Santa Cruz Biotechnology) overnight or control rabbit IgG. Immune complexes were precipitated with protein A agarose beads, washed, and eluted in 100 μl of TE with 0.5% SDS and 200 μg/ml proteinase K. Precipitated DNA was further purified by phenol/chloroform extraction and ethanol precipitation and analyzed by quantitative PCR (qPCR). The primers used to analyze Foxo1 binding to regulatory elements (Erag1–Erag3) in the *Rag1-Rag2* locus (17-20) were: Erag1, ACACCCTAAATGGGCCGTGAAC (5' primer) and CAGAACCCGAGGGCTTAGCATT (3' primer); Erag2, AACTTCCTCCAGCAGGCGATCT (5' primer) and ACCCATTTCCAAGCAGGAGAGG (3' primer); Erag3, AAGCCTCTCTTTGTACCCAACCTCAC (5' primer) and TTGACTGTCAGTTCAGCCAAAGGAAT (3' primer).

For *CDK4* amplification analysis**,** genomic DNA was obtained from frozen material of the lymphoma cases using proteinase K/RNase treatment and phenol/chloroform extraction. At least three replicates of 40 ng genomic DNA were subjected to qPCR analysis to assess *CDK4* copy number. Sequences of the *CDK4* detection probe and primers were followed the methods previously described (21, 22). *CDK4* –forward: 5′-CATGTAGACCAGGACCTAAGGACA-3 and *CDK4* reverse: 5′-GATCGTTTCGGCTGGCAA-3′.
The *CDK4* probe 5′-CTGGACAAGGCACCCCCACCA-3′ was labeled with 6-carboxyfluorescein as the reporter dye and 6-carboxytetramethylrhodamine as the quencher fluorescent and 3′ phosphorylated to prevent elongation during PCR be used for *CDK4* gene expression analysis. The primers and probe used in

the real-time PCR DNA *CDK4* copy number analyses were used for *CDK4* expression analysis as all the oligonucleotides were designed in an exonic region of the *CDK4* gene ((21).

Supplemental References

1. Schmitt, C.A., Fridman, J.S., Yang, M., Lee, S., Baranov, E., Hoffman, R.M., and Lowe, S.W. 2002. A senescence program controlled by p53 and p16INK4a contributes to the outcome of cancer therapy. *Cell* 109:335-346.
2. Huang, H., Regan, K.M., Lou, Z., Chen, J., and Tindall, D.J. 2006. CDK2-dependent phosphorylation of FOXO1 as an apoptotic response to DNA damage. *Science* 314:294-297.
3. Wang, E.S., Teruya-Feldstein, J., Wu, Y., Zhu, Z., Hicklin, D.J., and Moore, M.A. 2004. Targeting autocrine and paracrine VEGF receptor pathways inhibits human lymphoma xenografts in vivo. *Blood* 104:2893-2902.
4. Schmitz, R., Young, R.M., Ceribelli, M., Jhavar, S., Xiao, W., Zhang, M., Wright, G., Shaffer, A.L., Hodson, D.J., Buras, E., et al. 2012. Burkitt lymphoma pathogenesis and therapeutic targets from structural and functional genomics. *Nature* 490:116-120.
5. Leonard, J.P., LaCasce, A.S., Smith, M.R., Noy, A., Chirieac, L.R., Rodig, S.J., Yu, J.Q., Vallabhajosula, S., Schoder, H., English, P., et al. 2012. Selective CDK4/6 inhibition with tumor responses by PD0332991 in patients with mantle cell lymphoma. *Blood* 119:4597-4607.
6. Chiron, D., Martin, P., Di Liberto, M., Huang, X., Ely, S., Lannutti, B.J., Leonard, J.P., Mason, C.E., and Chen-Kiang, S. 2013. Induction of prolonged early G1 arrest by CDK4/CDK6 inhibition reprograms lymphoma cells for durable PI3Kdelta inhibition through PIK3IP1. *Cell Cycle* 12:1892-1900.
7. Huang, X., Di Liberto, M., Jayabalan, D., Liang, J., Ely, S., Bretz, J., Shaffer, A.L., 3rd, Louie, T., Chen, I., Randolph, S., et al. 2012. Prolonged early G(1) arrest by selective CDK4/CDK6 inhibition sensitizes myeloma cells to cytotoxic killing through cell cycle-coupled loss of IRF4. *Blood* 120:1095-1106.
8. Fry, D.W., Harvey, P.J., Keller, P.R., Elliott, W.L., Meade, M., Trachet, E., Albassam, M., Zheng, X., Leopold, W.R., Pryer, N.K., and Toogood, P.L. 2004. Specific inhibition of cyclin-dependent kinase 4/6 by PD 0332991 and associated antitumor activity in human tumor xenografts. *Mol. Cancer Therapeutics* 3:1427-1438.
9. Lewis, S.M., Agard, E., Suh, S., and Czyzyk, L. 1997. Cryptic signals and the fidelity of V(D)J joining. *Mol Cell Biol* 17:3125-3136.
10. Ramsden, D.A., McBlane, J.F., van Gent, D.C., and Gellert, M. 1996. Distinct DNA sequence and structure requirements for the two steps of V(D)J recombination signal cleavage. *Embo J* 15:3197-3206.
11. Isoda, T., Takagi, M., Piao, J., Nakagama, S., Sato, M., Masuda, K., Ikawa, T., Azuma, M., Morio, T., Kawamoto, H., et al. 2012. Process for immune defect and chromosomal translocation during early thymocyte development lacking ATM. *Blood* 120:789-799.
12. Sakata, J., Inoue, J., Ohi, H., Kosugi-Okano, H., Mishima, Y., Hatakeyama, K., Niwa, O., and Kominami, R. 2004. Involvement of V(D)J recombinase in the generation of intragenic deletions in the Rit1/Bcl11b tumor suppressor gene in gamma-ray-induced thymic lymphomas and in normal thymus of the mouse. *Carcinogenesis* 25:1069-1075.
13. Aplan, P.D., Lombardi, D.P., Ginsberg, A.M., Cossman, J., Bertness, V.L., and Kirsch, I.R. 1990. Disruption of the human SCL locus by "illegitimate" V-(D)-J recombinase activity. *Science* 250:1426-1429.
14. Kirsch, I.R., and Lista, F. 1997. Lymphocyte-specific genomic instability and risk of lymphoid malignancy. *Semin Immunol* 9:207-215.
15. van der Horst, A., and Burgering, B.M. 2007. Stressing the role of FoxO proteins in lifespan and disease. *Nat Rev Mol Cell Biol* 8:440-450.
16. Zou, X., Ray, D., Aziyu, A., Christov, K., Boiko, A.D., Gudkov, A.V., and Kiyokawa, H. 2002. Cdk4 disruption renders primary mouse cells resistant to oncogenic transformation, leading to Arf/p53-independent senescence. *Genes Dev* 16:2923-2934.
17. Dengler, H.S., Baracho, G.V., Omori, S.A., Bruckner, S., Arden, K.C., Castrillon, D.H., DePinho, R.A., and Rickert, R.C. 2008. Distinct functions for the transcription factor Foxo1 at various stages of B cell differentiation. *Nat Immunol* 9:1388-1398.
18. Schulz, D., Vassen, L., Chow, K.T., McWhirter, S.M., Amin, R.H., Moroy, T., and Schlissel, M.S. 2012. Gfi1b negatively regulates Rag expression directly and via the repression of FoxO1. *J Exp Med* 209:187-199.
19. Ochiai, K., Maienschein-Cline, M., Mandal, M., Triggs, J.R., Bertolino, E., Sciammas, R., Dinner, A.R., Clark, M.R., and Singh, H. 2012. A self-reinforcing regulatory network triggered by limiting IL-7 activates pre-BCR signaling and differentiation. *Nat Immunol* 13:300-307.
20. Herzog, S., Reth, M., and Jumaa, H. 2009. Regulation of B-cell proliferation and differentiation by pre-B-cell

receptor signalling. *Nat Rev Immunol* 9:195-205.
21. Hernandez, L., Bea, S., Pinyol, M., Ott, G., Katzenberger, T., Rosenwald, A., Bosch, F., Lopez-Guillermo, A., Delabie, J., Colomer, D., et al. 2005. CDK4 and MDM2 gene alterations mainly occur in highly proliferative and aggressive mantle cell lymphomas with wild-type INK4a/ARF locus. *Cancer Res* 65:2199-2206.
22. Al-Assar, O., Rees-Unwin, K.S., Menasce, L.P., Hough, R.E., Goepel, J.R., Hammond, D.W., and Hancock, B.W. 2006. Transformed diffuse large B-cell lymphomas with gains of the discontinuous 12q12-14 amplicon display concurrent deregulation of CDK2, CDK4 and GADD153 genes. *Br J Haematol* 133:612-621.